^{68}Ga-PSMA PET/CT and Volumetric Morphology of PET-Positive Lymph Nodes Stratified by Tumor Differentiation of Prostate Cancer

Maria Vinsensia[1], Peter L. Chyoke[2], Boris Hadaschik[3,4], Tim Holland-Letz[5], Jan Moltz[6], Klaus Kopka[7], Isabel Rauscher[8], Walter Mier[1], Markus Schwaiger[8], Uwe Haberkorn[1,9], Tobias Mauer[10], Clemens Kratochwil[1], Matthias Eiber*[8,11], and Frederik L. Giesel*[1,9]

[1]Department of Nuclear Medicine, University Hospital Heidelberg, Heidelberg, Germany; [2]Molecular Imaging Program, National Institutes of Health, Bethesda, Maryland; [3]Department of Urology, University Hospital Heidelberg, Heidelberg, Germany; [4]Department of Urology, University Hospital Essen, Essen, Germany; [5]Department of Biostatistics, German Cancer Research Center (DKFZ), Heidelberg, Germany; [6]Fraunhofer MEVIS, Bremen, Germany; [7]Radiopharmaceutical Chemistry, German Cancer Research Center (DKFZ), Heidelberg, Germany; [8]Department of Nuclear Medicine, Klinikum Rechts der Isar, Technical University of Munich, Munich, Germany; [9]Department of Molecular and Medical Pharmacology Cooperation Unit Nuclear Medicine (DKFZ), Heidelberg, Germany; [10]Clinical Cooperation Unit Nuclear Medicine, German Cancer Research Center (DKFZ), Heidelberg, Germany; and [11]Department of Molecular and Medical Pharmacology, David Geffen School of Medicine at UCLA, Los Angeles, California

^{68}Ga-prostate-specific membrane antigen (PSMA) PET/CT is a new method to detect early nodal metastases in patients with biochemical relapse of prostate cancer. In this retrospective investigation, the dimensions, volume, localization, and SUV_{max} of nodes identified by ^{68}Ga-PSMA were correlated to their Gleason score (GS) at diagnosis. **Methods:** All PET/CT images were acquired 60 ± 10 min after intravenous injection of ^{68}Ga-PSMA (mean dose, 176 MBq). In 147 prostate cancer patients (mean age, 68 y; range, 44–87 y) with prostate-specific antigen relapse (mean prostate-specific antigen level, 5 ng/mL; range, 0.25–294 ng/mL), 362 ^{68}Ga-PSMA PET–positive lymph nodes (LNs) were identified. These patients were classified on the basis of their histopathology at primary diagnosis into either low- (GS ≤ 6, well differentiated), intermediate- (GS = 7, moderately differentiated), or high-GS cohorts (GS ≥ 8, poorly differentiated prostate cancer). Using semiautomated LN segmentation software (Fraunhofer MEVIS), we measured node volume and short-axis dimensions (SADs) and long-axis dimensions based on CT and compared with the SUV_{max}. Nodes demonstrating uptake of ^{68}Ga-PSMA with an SUV_{max} of 2.0 or more were considered PSMA-positive, and nodes with an SAD of 8 mm or more were considered positive by morphologic criteria. **Results:** Mean SUV_{max} was 13.5 (95% confidence interval [CI], 10.9–16.1), 12.4 (95% CI, 9.9–14.9), and 17.8 (95% CI, 15.4–20.3) within the low-, intermediate-, and high-GS groups, respectively. The morphologic assessment of the ^{68}Ga-PSMA–positive LN demonstrated that the low-GS cohort presented with smaller ^{68}Ga-PSMA–positive LNs (mean SAD, 7.7 mm; n = 113), followed by intermediate- (mean SAD, 9.4 mm; n = 122) and high-GS cohorts (mean SAD, 9.5 mm; n = 127). On the basis of the CT morphology criteria, only 34% of low-GS patients, 56% of intermediate-GS patients, and 53% of high-GS patients were considered CT positive. Overall, ^{68}Ga-PSMA imaging led to a reclassification of stage in 90 patients (61%) from cN0 to cN1 over CT. **Conclusion:** ^{68}Ga-PSMA PET is a promising modality in biochemical recurrent prostate cancer patients for N staging. Conventional imaging underestimates LN involvement compared with PSMA molecular staging score in each GS cohort. The sensitivity of ^{68}Ga-PSMA PET/CT enables earlier detection of subcentimeter LN metastases in the biochemical recurrence setting.

Key Words: PSMA PET/CT; morphology; N-staging; lymph node; prostate cancer

J Nucl Med 2017; 58:1949–1955
DOI: 10.2967/jnumed.116.185033

Biochemical recurrence (BCR) of prostate cancer (PCa) after initial therapy can herald an aggressive disease course. About 1 in 3 PCa patients who underwent local treatment with curative intent develops prostate-specific antigen (PSA) recurrence within 15 y (*1,2*). PSA is a highly sensitive method for detecting recurrence, and treatment of BCR is critical to prolong survival (*3*). However, recurrences can occur in a variety of locations including the lymphatic tissue (30.5%), skeleton (42.1%), retroperitoneum (13.7%), and viscera (13.7%) (*4*). Treatment varies according to the number and site of recurrence, but localizing such recurrences has been problematic with existing imaging methods such as CT and bone scanning because of their lack of sensitivity and specificity. For instance, only 11%–14% of patients with biochemical failure after radical prostatectomy have positive CT scan findings (*5,6*), with similar results with MRI (*6–8*). Therefore, detecting and localizing sites of recurrence is a strong unmet need for personalizing salvage therapy within individual patients.

Although a variety of PET agents have been developed to detect PCa recurrences, the most successful to date have been small-molecule agents targeting prostate-specific membrane antigen (PSMA) (*9,10*). One such agent, Glu-urea-Lys-(Ahx)-(^{68}Ga(HBED-CC)), also known as ^{68}Ga-PSMA, is particularly promising (*10–12*).

Received Nov. 15, 2016; revision accepted May 5, 2017.
For correspondence or reprints contact: Frederik L. Giesel, Department of Nuclear Medicine, University Hospital Heidelberg, INF 400 69120 Heidelberg, Germany.
E-mail: frederik@egiesel.com
*Contributed equally to this work.
Published online Jun. 21, 2017.

^{68}Ga-PSMA PET imaging has been shown to improve detection of lymph node metastasis and other sites of recurrence with very high positive predictive values and accuracy (*10,13,14*). Even though PET has a lower intrinsic spatial resolution of 3–5 mm compared with the submillimeter resolution for CT and MRI, ^{68}Ga-PSMA PET imaging has successfully detected nodal recurrences in two thirds of patients who would have been missed using conventional CT morphologic criteria (*15*). ^{68}Ga-PSMA PET/CT specifically benefits from the power of molecular imaging to detect small-sized but high–target-expressing lesions. One recent study demonstrated that ^{68}Ga-PSMA PET can achieve a sensitivity, specificity, and accuracy of 77.9%, 97.3%, and 89.9% for N staging in recurrent disease (*13*). A metaanalysis involving 16 ^{68}Ga-PSMA PET articles covering 1,309 patients reported a summary sensitivity and specificity of 80% and 97% on a per-lesion analysis (*14*).

Until now, most ^{68}Ga-PSMA PET imaging studies have focused on the occurrence of lymph node metastases without correlation to the risk profile of the patient at primary diagnosis. For instance, the performance of ^{68}Ga-PSMA PET studies in PCa patients with histopathologic low-risk disease is still lacking. Thus, the aim of this study was to compare the profiles of ^{68}Ga-PSMA PET–positive nodal metastases in patients with BCR according to PSMA uptake and CT on well, moderately, and poorly differentiated PCa at initial diagnosis.

MATERIALS AND METHODS

Patients

In this 2-center retrospective investigation, we evaluated 362 PET-positive lymph nodes in 147 consecutive patients (median age, 68 y; range, 44–87 y) with BCR of PCa (median PSA, 5 ng/mL; range, 0.2–294 ng/mL). The analysis was based on institutional databases at the University of Heidelberg and the Technical University Munich, which was randomized to reach a relatively equal cohort size. Only patients who underwent previous prostatectomy without any other oncologic disease were included in this study. Gleason scores (GS) were obtained according to the reports on prostatectomy specimen, and because of the restriction of data low-GS patients' grading was based on either prostatectomy specimen or biopsy. Of 51 low-GS patients, grading for 32 GS was based on prostatectomy specimen and grading for 19 GS was based on biopsy. BCR was defined as 2 sequential PSA values of 0.2 ng/mL or more after prostatectomy (*3*). Patient characteristics are shown in Table 1. Before prostatectomy, the median PSA was 13 ng/mL (range, 2–252 ng/mL). Patients were stratified by GS as follows: low-GS (GS $\leq$ 6, well-differentiated PCa), intermediate-GS (GS = 7, moderately differentiated PCa), or high-GS cohort (GS $\geq$ 8, poorly differentiated PCa). All patients were enrolled under an investigational protocol that was approved by the investigational review board of both universities and was in accordance with the Helsinki Declaration (permit S-321/12 at the University of Heidelberg and 5665/13 at the Technical University Munich). Written informed consent for anonymized evaluation and publication of their data were obtained from all patients.

Image Acquisition, PSMA PET Analysis, and Volumetric CT Histogram Analysis

All PET/CT examinations were performed on a Biograph 6 PET/CT or a Biograph mCT scanner (Siemens Medical Solutions). Imaging was initiated 60 $\pm$ 10 min after intravenous injection of ^{68}Ga-PSMA at a median dose of 2–3 MBq/kg of body weight. On the Biograph 6 PET/CT, a CT (130 keV, 80 mAs; CareDose) without contrast medium was obtained for attenuation correction of the PET scan. On the Biograph mCT, first a diagnostic CT scan was obtained in the portal venous phase 80 s after intravenous injection of contrast agent (Imeron 300; Bracco Imaging) followed by the PET scan.

TABLE 1
Patient Characteristics

Patient characteristic	*n*
Total no. of patients	147
Low-GS cohort	
No. of patients	51
Median age (y)	71 (59–87)
GS	6
Median iPSA (ng/mL)	11.3 (3.2–84.3)
Median BCR PSA (ng/mL)	5.0 (0.5–41.3)
Mean time interval from RP to BCR (mo)	103
Further treatment	
Radiation therapy after RP	5
Androgen-deprivation therapy during/prior imaging	4
Unknown	20
Intermediate-GS cohort	
No. of patients	48
Median age (y)	66 (52–85)
GS	7
Median iPSA (ng/mL)	12.0 (3.8–252.0)
Median BCR PSA (ng/mL)	5.1 (0.3–212.0)
Mean time interval from RP to BCR (mo)	56
Further treatment	
Radiation therapy after RP	20
Androgen-deprivation therapy during/prior imaging	12
Unknown	6
High-GS cohort	
No. of patients	48
Median age (y)	66 (44–80)
GS	$\geq$ 8
Median iPSA (ng/mL)	23.5 (2–241)
Median BCR PSA (ng/mL)	5.0 (0.2–293.7)
Mean time interval from RP to BCR (mo)	45
Further treatment	
Radiation therapy after RP	15
Androgen-deprivation therapy during/prior imaging	18
Unknown	8

RP = radical prostatectomy.
Data in parentheses are ranges.

Static emission scans, corrected for dead time, scatter, and decay, were acquired from the vertex to the proximal legs—requiring 8 bed positions, each taking 3–4 min. The images were iteratively reconstructed with an ordered-subset expectation maximization algorithm using 4 iterations with 8 subsets and gaussian filtering with an in-plane spatial resolution of 5 mm in full width at half maximum. For

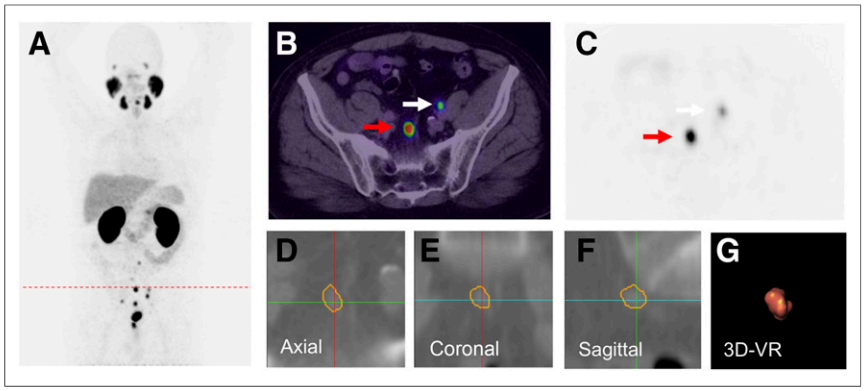

FIGURE 1. A 66-y-old patient with PSA relapse of 9.1 ng/mL, 5 y after radical prostatectomy (GS, 9; iPSA level, 69.9 ng/mL). (A) ^{68}Ga-PSMA PET maximum-intensity projection demonstrates multiple positive nodes in pelvic and abdominal region. (B) Single axial PET/CT image presents 2 PSMA-positive nodes (arrows). (C) Node indicated by red arrow with SUV_{max} 36.32 was segmented using Fraunhofer MEVIS software. The software enables automatic quantification of dimensions based on axial (D), coronal (E), and sagittal planes (F) of CT images (SAD, 7.57 mm; LAD, 11.35 mm; volume, 0.5 mL). (G) Image shows 3-dimensional volume rendering (VR), which was also provided by the software.

calculation of the SUV, circular regions of interest were drawn around the region of interest on transaxial slices and automatically adapted to a 3-dimensional volume of interest with e.soft software (Siemens) at a 70% isocontour. The CT scan was reconstructed with a B30 kernel to a slice thickness of 5 mm with an increment of 2.5 mm.

The threshold SUV_{max} for discriminating between benign and malignant lymph nodes in ^{68}Ga-PSMA PET was based on a blood-pool sample from 20 patients in each group and results from a recent prospective study in primary PCa evaluating the use of SUV thresholding (*15,16*). On these considerations, lymph nodes were considered abnormal if their uptake SUV exceeded 2.0. A maximum of 3 malignant nodes was identified in all patients. If a patient harbored more than 3 lymph node metastases, we chose the 3 most prominent lymph nodes with the highest SUV_{max} value as it represents PSMA uptake. All suspected lymph nodes were assigned to one of the following anatomic locations: regional lymph node metastasis including internal iliac, external iliac, obturator fossa, presacral, and distant lymph node metastasis for those around the common iliac, paraaortic, paracaval/interaortocaval, and other regions, for example, cervical and mediastinal (*17*).

Volumetric CT analysis was performed on ^{68}Ga-PSMA PET–positive nodes using semiautomated software (Fraunhofer MEVIS) that segments the nodes and automatically determines mean density, short-axis diameter (SAD), long-axis diameter (LAD), and volume (Figs. 1 and 2). Semiautomatic 3-dimensional histogram analysis was performed after the user provided a seed point in the lymph node and the software found the margins of the node. The segmentation started with a fixed-width thresholding around the seed point. To remove attached vessels, muscles, or other lymph nodes, a watershed transform was performed on the distance map of the thresholding result. The watershed transform is controlled to include and exclude features that are set according to an ellipsoid approximation of the lymph node. Quantitative and qualitative data of each patient were analyzed by 1 experienced radiologist and 1 nuclear medicine physician in each center. The volumes were evaluated by a radiologist to ensure that no extra nodal tissue was segmented and each node was manually corrected in all 3 dimensions, if necessary. The inter- and intraobserver reproducibility demonstrated a coefficient of variation of less than 5% (*18*). Any lymph node with an SAD above 8 mm was considered positive according to CT criteria (*7,8*). The size, represented by volume, SADs and LADs, and node location, was recorded for every node.

Statistical Evaluation

The evaluation of each group was based on the following parameters: measured SUV_{max}, volume, SAD, and LAD. To account for multiple observations within the same patients (up to 3 lymph nodes), comparisons between different risk cohorts were performed using a linear mixed model with risk group as a fixed effect and patient ID as a random effect. Descriptive statistics defining the percentage of positive PET/CT scans with nodes smaller than 8-mm SAD were performed. Statistical calculations were performed using the software SAS (Proc Mixed; SAS Institute) and IBM SPSS Statistics (IBM Corp.).

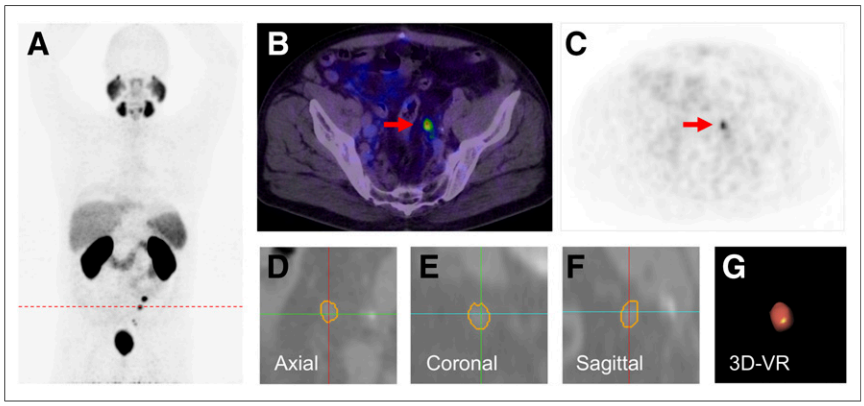

FIGURE 2. A 58-y-old patient with PSA relapse of 4.9 ng/mL, 9 mo after prostatectomy (GS, 6; iPSA, 10 ng/mL). (A) Patient presented multiple ^{68}Ga-PSMA PET–positive nodes as shown in PET maximum-intensity projection. (B and C) A positive node (red arrow) with PSMA uptake SUV_{max} 7.2 was segmented using Fraunhofer MEVIS software (SAD, 5.93 mm; LAD, 7.73 mm; and volume, 0.31 mL) Images (D–F) show segmented lymph node on each plane and volume rendering (VR) (G).

RESULTS

Among 147 patients with BCR, a total of 362 positive lymph nodes were evaluated on ^{68}Ga-PSMA PET/CT. The mean SUV_{max} of ^{68}Ga-PSMA uptake in malignant nodes was 14.67 (interquartile range, 11.0–17.0). One hundred thirteen lymph nodes in 51 low-GS patients, 122 lymph nodes in 48 intermediate-GS patients, and 127 lymph nodes in 48 high-GS patients were positive on ^{68}Ga-PSMA PET scans. Median initial PSA (iPSA) in the low-GS cohort was 11.3 ng/mL (range, 3.2–84.3 ng/mL), in the intermediate-GS cohort iPSA was 12.0 ng/mL (range, 3.8–252.0 ng/mL), and in the high-GS cohort iPSA was 23.5 ng/mL (range, 2.0–241.0 ng/mL).

TABLE 2
Mean SUV_{max}, SAD, LAD, and Volume Between Each Cohort

Risk profile	SUV_{max}			SAD (mm)			LAD (mm)			Volume (mL)		
	Mean	95% CI, lower	95% CI, upper	Mean	95% CI, lower	95% CI, upper	Mean	95% CI, lower	95% CI, upper	Mean	95% CI, lower	95% CI, upper
Low GS	13.5	10.9	16.1	7.7	6.9	8.4	11.9	11.0	12.7	1.0	0.8	1.2
Intermediate GS	12.4	9.9	14.9	9.4	8.6	10.2	13.9	12.8	14.9	1.6	1.1	2.2
High GS	17.8	15.4	20.3	9.5	8.7	10.4	14.2	13.1	15.2	1.7	1.1	2.3

Median PSA values at imaging were 5.0 ng/mL (range, 0.5–41.3 ng/mL), 5.1 ng/mL (range, 0.3–212 ng/mL), and 5.0 ng/mL (range, 0.2–293.7 ng/mL) for low-, intermediate-, and high-GS patients (Table 1).

^{68}Ga-PSMA Ligand Uptake

The ^{68}Ga-PSMA ligand uptake showed a nonsignificant difference between the 3 GS cohorts ($P = 0.062$). Mean SUV_{max} of affected lymph nodes in the low-, intermediate-, and high-GS cohorts was 13.5 (95% confidence interval [CI], 10.9–16.1), 12.4 (95% CI, 9.9–14.9), and 17.8 (95% CI, 15.4–20.3), respectively (Table 2; Fig. 3A). Although the P value of uptake between the intermediate- and high-GS cohorts was less than 0.05 ($P = 0.031$), it is considered nonsignificant because the P value of the mixed model of the 3 cohorts was 0.05 or more (Table 3).

Morphometric Analysis

The 3-dimensional volumetric segmentation enabled derivation of several important parameters: lymph node size represented by SAD and LAD and lymph node volume of ^{68}Ga-PSMA PET–positive findings. The SAD between GS cohorts demonstrated significant differences ($P = 0.013$) as follows: mean low-GS SAD, 7.7 mm (95% CI, 6.9–8.4 mm; $n = 113$); intermediate-GS SAD, 9.4 mm (95% CI, 8.6–10.2 mm; $n = 122$); and high-GS SAD, 9.5 mm (95% CI, 8.7–10.4 mm; $n = 127$) (Table 2; Fig. 3B). Pairwise comparisons for lymph node SADs showed a significant difference between low- and intermediate-GS cohorts ($P = 0.011$) and low- and high-GS lymph node SADs ($P = 0.009$) (Table 3). The difference in SAD between the intermediate- and high-GS cohorts was not significant. ^{68}Ga-PSMA–positive lymph nodes also showed differences in LAD ($P = 0.023$) according to GS cohort with a mean low-GS LAD of 11.9 mm (95% CI, 11.0–12.7 mm), mean intermediate-GS LAD of 13.9 mm (95% CI, 12.8–14.9 mm), and mean high-GS LAD of 14.2 mm (95% CI, 13.1–15.2 mm). However, as seen in Table 3, overall lymph node volumes were not significantly different among the 3 cohorts.

Among the 113 PSMA-positive lymph nodes (found in 31/51 patients) in the low-GS cohort, 75 (66%) were morphologically negative (≤8 mm) on CT and 38 (34%) were morphologically positive. In the intermediate-GS cohort, among 122 PSMA-positive lymph nodes, 53 (44%) were morphologically negative and 69 (56%) were morphologically positive. In the high-GS group, among 127 consecutive PSMA-positive lymph nodes, 60 (47%) nodes were morphologically negative and 67 (53%) were morphologically positive. Figure 4 depicts the morphologic distribution in each cohort next to the CT morphologic cutoff line of 8 and 10 mm. Therefore, among 362 PSMA-positive lymph nodes, 174 (48%) were positive based on conventional imaging criteria and 188 nodes (52%) were negative.

Staging Results by Imaging Modality

For each risk cohort, ^{68}Ga-PSMA PET/CT imaging demonstrated tumor detection superior to CT. Using standard TNM staging CT would have properly staged only 57 (38%) of 147 patients. By this standard, 35 patients (69%) of the low-GS cohort, 29 patients (60%) of the intermediate-GS cohort, and 26 patients (54%) of high-GS cohort would falsely be considered as cN0 by CT criteria. Overall, ^{68}Ga-PSMA PET/CT led to reclassification of 90 patients (61%) from cN0 to cN1.

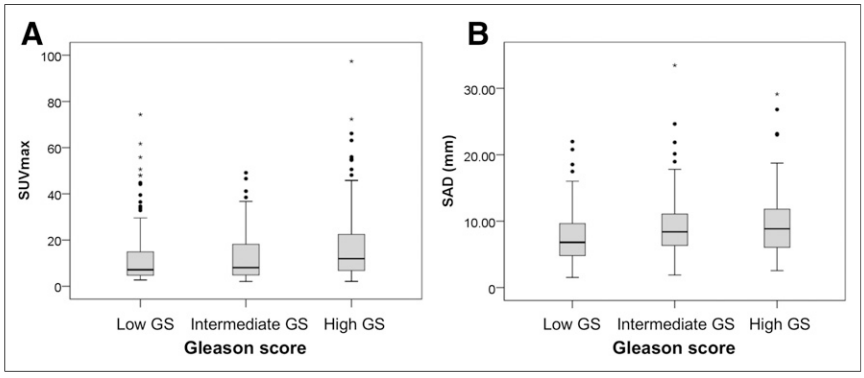

FIGURE 3. Uptake and morphologic distribution in each risk group. (A) ^{68}Ga-PSMA ligand uptake as represented with SUV_{max} shows increasing trend together with risk profile. (B) SAD of ^{68}Ga-PSMA–positive lymph node displays that most metastatic lymph nodes are smaller than 10 mm, indicating that ^{68}Ga-PSMA is able to detect micrometastasis. SAD shows growing tendency alongside risk profile.

Location of Lymph Nodes

Among the nodes detected by ^{68}Ga-PSMA PET, 254 (70%) were located in distant lymphatic stations (common iliac vessel, paraaortic, paracaval/interaortocaval, and other regions, for example, cervical and mediastinal), meanwhile 108 (30%) nodes were in regional, pelvic lymph node stations (internal iliac vessel, external iliac vessel, obturator fossa, and presacral). Distant ^{68}Ga-PSMA PET/CT–positive lymph nodes were found in 84% of low-GS patients, 68% of intermediate-GS patients, and 71% of high-GS patients. Regional nodes were found in 16%, 32%, and 29% of low-, intermediate-, and high-GS cohorts, respectively. The most

TABLE 3
Pairwise Comparisons Between Each Cohort

Risk profile (I*J)	Pairwise comparisons, *P**			
	SUV_{max}	SAD	LAD	Volume
Mixed-model, 3 groups	0.062	0.013*	0.023*	0.110
Low GS vs. intermediate GS	0.797	0.011*	0.024*	0.150
Intermediate GS vs. high GS	0.031	0.953	0.801	0.540
Low GS vs. high GS	0.057	0.009*	0.012*	0.040

*Mean difference is significant at 0.05 level.

common location for a distant malignant node was the paraaortic station (17%), followed by the interaortocaval and mediastinal regions.

DISCUSSION

In this study, we have shown that ^{68}Ga-PSMA PSMA PET imaging is superior to conventional CT criteria independent of initial tumor differentiation of PCa. ^{68}Ga-PSMA ligand uptake in patients with BCR may vary according to the GS of the patient. Multiple studies have shown that the sensitivity and specificity of ^{68}Ga-PSMA PET/CT varies from 54% to 94% and 97% to 100%, respectively (*10,12–15,19*). Because of ethical and practical reasons, histopathologic verification could be obtained only in 4 of 147 patients who underwent salvage lymphadenectomy after ^{68}Ga-PSMA PET. In all other patients, a comprehensive standard of reference including contrast-enhanced CT, MRI, repeated ^{68}Ga-PSMA ligand PET/CT, and course of PSA confirming the initial suggestive lesions or showing disappearance of suspected lesions after local/systemic treatment was obtained, also suggesting the malignancy nature of the detected nodes.

The ^{68}Ga-PSMA uptake increases with the initial risk profile of the patient. One potential confounder in this study would be other malignancies. Thyroid, colon, kidney, and brain malignancies have also shown PSMA uptake. Therefore, in this study we intentionally excluded patients with other oncologic disease to avoid these false-positive findings. Other studies have also reported possible false-positives in the cervical, celiac, and sacral ganglia (*20,21*). The SUV_{max} of ganglia, however, was relatively low compared with actual lymph nodes metastasis. Moreover, the localization of positive PSMA uptake corresponded to well-known lymph node stations, further lowering the possibility of a false-positive.

The morphologic distribution as shown in Figure 4 illustrates that nodal staging with CT alone strongly underestimates nodal involvement. Only 48% of all ^{68}Ga-PSMA PET/CT–positive nodes exceeded the size criteria for metastasis on CT. The CT sensitivity calculated in this study (48%) is consistent with the existing data published (*5,6*). In the low-GS cohort, most (66%) positive lymph nodes were smaller than 8 mm. Regardless of their small size, these nodes demonstrated excellent uptake, with a mean SUV_{max} of 13.5 (95% CI, 10.9–16.1). Though it is important for patient management to detect and localize the sites of recurrence as early as possible, cross-sectional imaging is known to be insufficient. Detecting the metastases while the lesions are still small may allow earlier and individually tailored salvage therapies (*3,22*). A comparison of 2 main parameters, ^{68}Ga-PSMA PET SUV_{max} and SAD on CT, is shown in Figure 5.

PCa patients with low initial GS are considered unlikely to recur but nonetheless do probably because of higher grade disease that is not diagnosed at biopsy. This is also 1 limitation of our study: 19 of 51 gradings were done by biopsy, which might translate into understaging by sampling error in comparison to histologic workup of the whole gland after prostatectomy. It is unclear whether PSMA PET on biochemical relapse is as useful in these low-GS patients as it is in higher GS patients who have a known likelihood of progression. Patients with local recurrence in the low-risk group typically respond well to early salvage radiotherapy (*23*). Therefore, the findings of this study might offer the possibility to further individualize salvage radiation and to possibly use targeted radiotherapy to recurrent lesions in the future, thus sparing unnecessary pelvic irradiation. We identified pelvic lymph node metastases in 61% of BCR patients with initial low-risk GS, which is well in line with recent literature that reported lymph node metastases as reason for BCR in 81% of patients using response to salvage radiotherapy as a standard of reference (*24*).

The localization of the nodal involvement is also essential to determine whether systemic or regional salvage treatments are required. ^{68}Ga-PSMA PET/CT imaging provides indispensable information about the location and number of metastases. In fact, because most patients had previous pelvic lymph node resections, most of the positive nodes (70%) in this study were located in more distant lymph stations. Thus, this kind of information could significantly affect potential radiation therapy planning similar to the results recently reported by van Leeuwen et al. (*25*).

Comparison of the 3 GS groups showed significant differences in the diameters (SAD and LAD) of detected nodes according to risk cohort. Although SAD and LAD should correlate with the volume, nodal

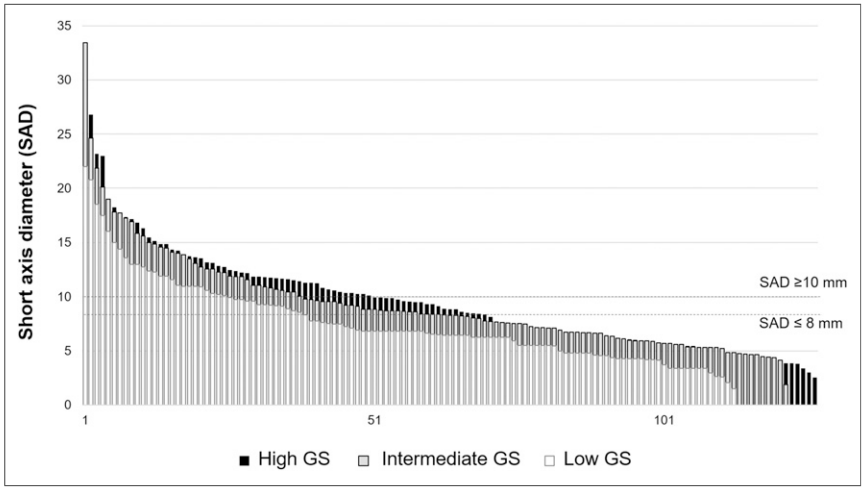

FIGURE 4. Morphologic distribution of all 362 lymph nodes aligned to their SAD. Cutoff SAD was set to both 10 and 8 mm. This graph demonstrates that around two thirds of PSMA-positive nodes are not sufficiently detected based on their morphologic criteria.

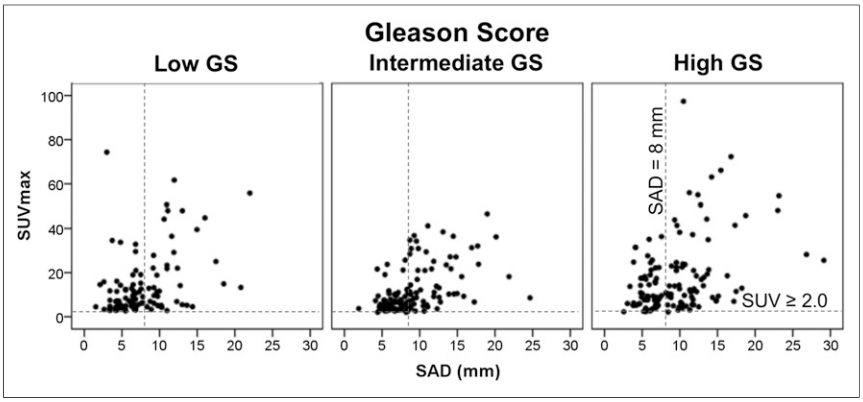

FIGURE 5. Relationship between SUV_{max} and SAD (mm). CT morphologic cutoff was set at 8 mm and PET/CT SUV_{max} at 2.0.

volume did not correlate well with risk correlation. It is possible that shape (reflected better as SAD and LAD) plays a more important role than volume per se. It is also possible that the software over- or underestimates volume whereas diameter determination is more readily verified. Furthermore, these results may also be an artifact of selecting only the 3 most prominent nodes in men with multiple metastases. The time interval of BCR corresponds with the risk profile of each cohort. BCR tends to occur for low-GS patients within the longest time interval of 103 mo, meanwhile for intermediate- and high-GS patients BCR occurred within 56 and 45 mo, respectively. In such cases, the BCR-free interval and SAD of lymph node metastases may indicate the tissue growth/malignancy of the metastases in each cohort. However, more research is needed to better understand the correlation between time interval and the malignancy of the metastases.

Our results are similar to previous studies. A ^{68}Ga-PSMA study of 53 positive lymph nodes in intermediate- and high-risk patients (GS $\geq$ 7) showed an SUV_{max} of 12.7 (range, 2.4–51.0) with a corresponding node size of 8.3 mm (range, 4–25 mm) (*13*). These data are in line with our evaluation of intermediate- and high-risk cohorts. In comparison, in this study the mean SUV_{max} was 12.4 (range, 2–49) and SAD was 9.4 mm (range, 1.9–33.5 mm) in the intermediate-risk group, and the mean SUV_{max} was 17.8 (range, 2–97) and SAD was 9.5 mm (range, 2.6–29.1 mm) in the high-risk cohort.

The classification of the subgroups in this study was based on the GS. The GS was determined at the initial PCa diagnosis, thus making its relevance in a recurrence or relapse situation questionable because the patient has received prostatectomy or other therapy. However, the correlation of GS and the risk of recurrent PCa has been reported in various studies (*26*,*27*). The guidelines on PCa published by the European Association of Urology, for instance, use the classification of GS (at biopsy) as a predictor of biochemical relapse (*3*). However, there have been some modifications regarding the definition of GS 6, which upgraded the previous classification of Gleason 6 into Gleason 7a (*26*). Some patients in this study were diagnosed before 2010, thus the Gleason grading reported may not be equal with the current definition. Overall, using the GS makes our results more generalizable.

Despite the retrospective nature of this study, randomized patient selection within each GS cohort and masked analysis might help in reducing unforeseen biases. The selection of the 3 most prominent ^{68}Ga-PSMA–positive lymph nodes from each patient might tend to overestimate the SUV_{max} and lesion volumes of each group, but at the same time reduce the in-patient uptake bias. The lack of routine histologic validation is 1 limitation of this study; however, after BCR surgery is rarely an option and clinical follow-up or imaging are routinely used standards of reference in this setting.

^{68}Ga-PSMA PET/CT is promising as a better restaging modality for PCa patient with PSA relapse. A further investigation with a better differentiation of the recurrence subgroup could provide a more refined indication of the size and SUV_{max} of lymph nodes as a function of assigned risk stratification. Besides GS, other relevant parameters such as PSA doubling time, tumor invasion specimen (pT stage), and time to PSA recurrence are intriguing and could provide a better specification for patient management. However, recently developed ^{18}F-labeled PSMA ligands allow a higher patient throughput and show promising PSMA diagnostics for both T and N/M staging in a urooncologic environment (*28–31*).

CONCLUSION

This retrospective study demonstrates that ^{68}Ga-PSMA PET imaging is clearly superior to CT for detecting recurrent nodal disease independently of initial histology. Within risk strata established at diagnosis, there are subtle differences both in uptake and in node diameters according to initial GSs. The ability of ^{68}Ga-PSMA PET/CT to better stage recurrent disease along with its ability to pinpoint metastatic sites make it a valuable tool in assessing patients with BCR regardless of the initial risk cohort.

DISCLOSURE

No potential conflict of interest relevant to this article was reported.

REFERENCES

1. Moschini M, Sharma V, Zattoni F, et al. Natural history of clinical recurrence patterns of lymph node-positive prostate cancer after radical prostatectomy. *Eur Urol.* 2016;69:135–142.
2. Freedland SJ, Presti JC Jr, Amling CL, et al. Time trends in biochemical recurrence after radical prostatectomy: results of the SEARCH database. *Urology.* 2003;61:736–741.
3. Mottet N, Bellmunt J, Briers E, et al. Guidelines on prostate cancer. European Association of Urology website. https://uroweb.org/wp-content/uploads/09-Prostate-Cancer_LR.pdf. 2015. Accessed July 27, 2016.
4. Nini A, Gandaglia G, Fossati N, et al. Patterns of clinical recurrence of node-positive prostate cancer and impact on long-term survival. *Eur Urol.* 2015;68:777–784.
5. Engeler CE, Wasserman NF, Zhang G. Preoperative assessment of prostatic carcinoma by computerized tomography weaknesses and new perspectives. *Urology.* 1992;40:346–350.
6. Hövels AM, Heesakkers RA, Adang EM, et al. The diagnostic accuracy of CT and MRI in the staging of pelvic lymph nodes in patients with prostate cancer: a meta-analysis. *Clin Radiol.* 2008;63:387–395.
7. Park SY, Oh YT, Jung DC, et al. Prediction of micrometastasis (<1 cm) to pelvic lymph nodes in prostate cancer: role of preoperative MRI. *AJR.* 2015;205:W328–W334.
8. McMahon CJ, Rofsky NM, Pedrosa I. Lymphatic metastases from pelvic tumors: anatomic classification, characterization and staging. *Radiology.* 2010;254:31–46.
9. Eder M, Eisenhut M, Babich J, et al. PSMA as a target for radiolabelled small molecules. *Eur J Nucl Med Mol Imaging.* 2013;40:819–823.

10. Afshar-Oromieh A, Avtzi E, Giesel FL, et al. The diagnostic value of PET/CT imaging with the ^{68}Ga-labelled PSMA ligand HBED-CC in the diagnosis of recurrent prostate cancer. *Eur J Nucl Med Mol Imaging.* 2015;42:197–209.
11. Eder M, Schäfer M, Bauder-Wüst U, et al. ^{68}Ga-complex lipophilicity and the targeting property of a urea-based PSMA inhibitor for PET imaging. *Bioconjug Chem.* 2012;23:688–697.
12. Eiber M, Maurer T, Souvatzoglou M, et al. Evaluation of hybrid ^{68}Ga-PSMA ligand PET/CT in 248 patients with biochemical recurrence after radical prostatectomy. *J Nucl Med.* 2015;56:668–674.
13. Rauscher I, Maurer T, Beer AJ, et al. Value of ^{68}Ga-PSMA HBED-CC PET for the assessment of lymph node metastases in prostate cancer patients with biochemical recurrence: comparison with histopathology after salvage lymphadenectomy. *J Nucl Med.* 2016;57:1713–1719.
14. Perera M, Papa N, Christidis D, et al. Sensitivity, specificity, and predictors of positive ^{68}Ga-prostate-specific membrane antigen positron emission tomography in advanced prostate cancer: a systematic review and meta-analysis. *Eur Urol.* 2016;70:926–937.
15. van Leeuwen PJ, Emmett L, Ho B, et al. Prospective evaluation of ^{68}gallium-PSMA positron emission tomography/computerized tomography for preoperative lymph node staging in prostate cancer. *BJU Int.* 2017;119:209–215.
16. Giesel FL, Fiedler H, Stefanova M, et al. PSMA PET/CT with Glu-urea-Lys-(Ahx)-(^{68}Ga(HBED-CC)) versus 3D CT volumetric lymph node assessment in recurrent prostate cancer. *Eur J Nucl Med Mol Imaging.* 2015;42:1794–1800.
17. Edge SB, Byrd DR, eds. *AJCC Cancer Staging Manual.* 7th ed. New York, NY: Springer; 2010.
18. Moltz JM, Bornemann L, Kuhnigk JM, et al. Advanced segmentation techniques for lung nodules, liver metastases, and enlarged lymph nodes in CT scans. *IEEE Processing.* 2009;3:122–134.
19. Hijazi S, Meller B, Leitsmann C, et al. Pelvic lymph node dissection for nodal oligometastatic prostate cancer detected by ^{68}Ga-PSMA-positron emission tomography/computerized tomography. *Prostate.* 2015;75:1934–1940.
20. Krohn T, Verburg FA, Pufe T, et al. (^{68}Ga)PSMA-HBED uptake mimicking lymph node metastasis in coeliac ganglia: an important pitfall in clinical practice. *Eur J Nucl Med Mol Imaging.* 2015;42:210–214.
21. Christoph R, Shozo O, Philipp M, et al. ^{68}Ga-PSMA-HBED-CC ligand uptake in cervical, coeliac and sacral ganglia as an important pitfall in prostate cancer PET imaging [abstract]. *J Nucl Med.* 2016;57(suppl 2):517.
22. Maurer T, Weirich G, Schottelius M, et al. Prostate-specific membrane antigen-radioguided surgery for metastatic lymph nodes in prostate cancer. *Eur Urol.* 2015;68:530–534.
23. Briganti A, Karnes RJ, Joniau S, et al. Prediction of outcome following early salvage radiotherapy among patients with biochemical recurrence after radical prostatectomy. *Eur Urol.* 2014;66:479–486.
24. Wenger H, Weiner AB, Razmaria A, Paner GP, Eggener SE. Risk of lymph node metastases in pathological Gleason score <6 prostate adenocarcinoma: analysis of institutional and population-based databases. *Urol Oncol.* 2017;35:31.e1–31.e6.
25. van Leeuwen PJ, Stricker P, Hruby G, et al. ^{68}Ga-PSMA has a high detection rate of prostate cancer recurrence outside the prostatic fossa in patients being considered for salvage radiation treatment. *BJU Int.* 2016;117:732–739.
26. Lucca I, Shariat SF, Briganti A, et al. Validation of tertiary Gleason pattern 5 in Gleason score 7 prostate cancer as an independent predictor of biochemical recurrence and development of a prognostic model. *Urol Oncol.* 2015;33:71.
27. Pierorazio PM, Walsh PC, Partin AW, et al. Prognostic Gleason grade grouping: data based on the modified Gleason scoring system. *BJU Int.* 2013;111:753–760.
28. Epstein JI, Egevad L, Amin MB. Grading Committee. The 2014 International Society of Urological Pathology (ISUP) consensus conference on Gleason grading of prostatic carcinoma: definition of grading patterns and proposal for a new grading system. *Am J Surg Pathol.* 2016;40:244–252.
29. Szabo Z, Mena E, Rowe SP, et al. Initial evaluation of [^{18}F]DCFPyL for prostate-specific membrane antigen (PSMA)-targeted PET imaging of prostate cancer. *Mol Imaging Biol.* 2015;17:565–574.
30. Giesel FL, Hadaschik B, Cardinale J, et al. F-18 labelled PSMA-1007: biodistribution, radiation dosimetry and histopathological validation of tumor lesions in prostate cancer patients. *Eur J Nucl Med Mol Imaging.* 2017;44:678–688.
31. Giesel FL, Kesch C, Yun J, et al. ^{18}F-PSMA-1007 PET/CT detects micrometastases in a patient with biochemically recurrent prostate cancer. *Clin Genitourin Cancer.* 2017;15:e497–e499.